Desalination and Water Treatment
www.deswater.com

doi: 10.1080/19443994.2016.1152646

57 (2016) 24574–24582
November

Taylor & Francis
Taylor & Francis Group

Corrected normalized permeate flux for a statistics-based fouling detection method in seawater reverse osmosis process

Minseok Kim[a], Beomseok Park[a], Young-Joo Lee[b], Jae-Lim Lim[b], Sangho Lee[a], Suhan Kim[a,*]

[a]*Department of Civil Engineering, Pukyong National University, 45 Yongso-ro, Nam-gu, Busan 608-737, Korea, emails: minseok9928@gmail.com (M. Kim), beomseok8612@gmail.com (B. Park), peterlee@pknu.ac.kr (S. Lee), Tel. +82 51 629 6065; Fax: +82 51 629 6063; email: suhankim@pknu.ac.kr (S. Kim)*
[b]*Water management & Research Center, K-Water Institute, 125, Yuseong-daero 1689, Yusong-Gu, Daejeon, Korea, emails: yjlee1947@kwater.or.kr (Y.-J. Lee), jllim@kwater.or.kr (J.-L. Lim)*

Received 23 October 2015; Accepted 8 January 2016

ABSTRACT

In the real-field application, the operation conditions for seawater reverse osmosis (SWRO) processes such as pressure, temperature, recovery rate, and feed concentration vary, which changes the permeate flow rate with no fouling. In order to detect fouling from the fluctuating permeate flow rates due to various operation conditions, they should be normalized. However, the normalization method using ASTM D4516 method still produces the fluctuation in the normalized permeate flow due to poor selections of osmotic pressure and temperature correction factor (TCF) equations, which do not reflect the characteristics of feed water and reverse osmosis membrane in the field very well. This work introduces the corrected normalized permeate flux (NPF) using the fitted osmotic pressure and TCF equations to minimize the fluctuation during a non-fouling situation and suggests a statistical approach to detect fouling by comparing the mean values of two groups with different variances. The laboratory-scale SWRO experiments with randomly changing operation conditions verify that the corrected NPF and the statistics-based fouling detection method works very well to find the early stage of fouling by humic acid. In addition, the fitted TCF equation affects the performance of the fouling detection method more than the fitted osmotic pressure equation.

Keywords: Seawater reverse osmosis (SWRO); Normalization; Corrected normalized permeate flux; Statistics-based fouling detection method

*Corresponding author.

Presented at 2015 Academic Workshop for Desalination Technology held in the Institute for Far Eastern Studies Seoul, Korea, 23 October 2015

1. Introduction

The water shortage is one of the biggest issues in the modern era. As the population increases to more than 7 billion, water demand has been increasing accordingly. Thus, seawater is considered as an important water source to meet the increasing water demand [1,2]. Recently, reverse osmosis (RO) process has become one of the most popular desalination technologies [3], and seawater reverse osmosis (SWRO) process dominates current desalination markets due to its lower cost compared to other desalination processes such as thermal distillation [4–6].

RO is a pressure-driven membrane process where solutes are separated from a solution by a semi-permeable membrane under a hydraulic pressure greater than the osmotic pressure of the solutes. It operates at ambient temperature without phase change, which makes it a relatively simple and versatile separation process [7]. One of the most challenging issues operating the RO processes is membrane fouling [8–16].

RO membrane fouling can be defined as a decline in performance due to foulants accumulation on the membrane surface [3], which is the result of the interfacial interactions between foulants and membrane surface (or fouling layer covered on the membrane surface) [11,12,15]. The fouling induces massive pretreatment, high operating pressures, and frequent chemical cleanings (which possibly damage membranes) to increase water cost [3,16]. Potential causes of the fouling include inorganic fouling (scaling), organic fouling, colloidal fouling, and biofouling [8]. The RO fouling mechanism is often complicated due to the interplay between the salt concentration polarization layer and the fouling layer on the membrane surface, which is called cake-enhanced osmotic pressure or cake-enhanced concentration polarization effect [10,14]. The fouling is influenced by operating conditions, solution chemistry, temperature, membrane properties, and module geometry, while biofilm formation is additionally governed by the biofouling potential of feed water [3,13].

Effective fouling control requires a good diagnosis of RO plant performance [8]. Fouling can be quantified by monitoring the RO membrane permeability (product flow rate per unit pressure). However, the RO membrane permeability is affected by not only fouling but also the feed–brine osmotic pressure and the feed water viscosity, which are influenced by feed concentration, temperature, and the recovery rate. During the operation of the RO processes, pressure, temperature, recovery rate, and feed concentration can vary. For example, a feed temperature drop of 4˚C normally causes a permeate flux decline of ~10% without any fouling effect. In order to distinguish the fouling effect from a normal phenomenon (i.e. non-fouling state), the measured permeate flow should be normalized such as ASTM D4516 method [17]. Normalization (or standardization) can be defined as a comparison of the actual performance to a given reference performance while the influences of operating parameters are considered.

However, the normalization using ASTM D4516 method is still not enough to detect the membrane fouling due to variance in the normalized data [18,19]. Field experiences for the past decades reported that it was extremely difficult to detect the early stage of the RO fouling by monitoring a long-term normalized data [18]. The main reasons why the normalization failed to detect the fouling easily could be the arbitrary selection of the empirical equations for the feed–brine osmotic pressure and temperature correction factor (TCF), which should be considered as the site-specific parameters. The hypothesis in this work is that the early fouling detection can be possible by selecting proper osmotic pressure and TCF equations, followed by a statistical approach to compare the mean values of two groups with different variances [20]. The objective of this work is to develop a statistics-based fouling detection method using corrected normalized permeate flux (NPF) calculated from the fitted osmotic pressure and TCF equations reflecting the characteristics of feed water and RO membrane. Laboratory-scale SWRO fouling tests with varying operation conditions will verify the developed fouling detection method.

2. Methods

2.1. Calculation and correction of NPF

Normalization is a comparison of the actual performance to a given reference performance while the influences of operating parameters (e.g. pressure, temperature, recovery rate, and feed concentration) are taken into account [17]. It involves referring the plant operation back to a standard condition, which can be defined as the operation condition when the RO plant shows the reference performance [19]. The reference performance may be the designed performance or the measured initial performance. Normalization with reference to the designed system performance is useful to verify that the plant gives the specified performance, while normalization with reference to initial system performance is useful to show up any performance change between day one and the actual date [19]. Among several normalized (or standardized) parameters, this work focuses on normalized permeate

flow, which is the permeate flow at a standard condition calculated using Eq. (1) suggested by ASTM D4516 [21]:

$$Q_{ps} = \frac{\left[P_{ps} - \frac{\Delta P_{fbs}}{2} - P_{ps} - \pi_{fbs} + \pi_{ps}\right](TCF_s)}{\left[P_{pa} - \frac{\Delta P_{fba}}{2} - P_{pa} - \pi_{fba} + \pi_{pa}\right](TCF_a)}(Q_{pa}) \quad (1)$$

where Q_{pa} = permeate flow at actual conditions, Q_{ps} = permeate flow at standard conditions (normalized permeate flow), P_{fa} = feed pressure at actual conditions (kPa), P_{fs} = permeate pressure at standard conditions (kPa), P_{pa} = permeate pressure at actual conditions (kPa), P_{ps} = permeate pressure at standard conditions (kPa), $\Delta P_{fba}/2$ = one half device pressure drop at actual conditions (kPa), $\Delta P_{fbs}/2$ = one half device pressure drop at standard conditions (kPa), π_{fba} = feed–brine osmotic pressure at actual conditions (kPa), π_{fbs} = feed–brine osmotic pressure at standard conditions (kPa), π_{pa} = permeate osmotic pressure at actual conditions (kPa), π_{ps} = permeate osmotic pressure at standard conditions (kPa), TCF_a = temperature correction factor at actual conditions, and TCF_s = temperature correction factor at standard conditions.

Eq. (1) can be applied to RO plants of a single or a multi-element system using hollow-fiber or spiral wound RO elements. Since laboratory-scale fouling data will be analyzed in this work, the characteristics of feed and brine are almost the same. Thus, the NPF with more simplified formula than Eq. (1) is introduced:

$$NPF = J_s = \frac{TCF_s(P_{fs} - \pi_{fs})}{TCF_a(P_{fa} - \pi_{fa})}(J_a) \quad (2)$$

where J_a = permeate flux (LMH) at actual conditions, J_s = permeate flux (LMH) at standard conditions (i.e. NPF), π_{fa} = feed osmotic pressure at actual conditions (kPa), and π_{fs} = feed osmotic pressure at standard conditions (kPa).

TCF is generally affected by the RO membrane and it is ideal to obtain TCF from the membrane manufactures. If unavailable, TCF can be calculated using a membrane-independent equation (TCF_1) [21]:

$$TCF_1 = 1.03^{(T-25)} \quad (3)$$

where T is temperature (°C). If the effect of membrane is considered, TCF can be calculated using a membrane-dependent equation (TCF_2) [17]:

$$TCF_2 = \exp\left[a \times \left(\frac{1}{298} - \frac{1}{T+273}\right)\right] \quad (4)$$

where a is the temperature coefficient for water transport of the RO membrane [13], which can be provided by the membrane manufacturer.

For the osmotic pressure, various empirical equations are available in literatures [17,21,22] such as:

$$\pi_1 = 0.2654\, C_f(T+273)/(1000 - C_f/1000) \quad (5)$$

$$\pi_2 = \frac{C_f(T+320)}{491000} \quad \text{for} \quad C_f < 20000 \text{ mg/l} \quad (6a)$$

$$\pi_2 = \frac{0.0117\, C_f - 34}{14.23} \cdot \frac{T+320}{345} \quad \text{for} \quad C_f > 20000 \text{ mg/l} \quad (6b)$$

$$\pi_3 = 0.00076\, C_f \quad (7)$$

where π_1, π_2, and π_3 are the empirical osmotic pressure equations, and C_f is feed concentration (mg/l).

NPF is calculated using Eq. (2) with a selected osmotic pressure equation from various candidates such as Eqs. (5)–(7) and a selected TCF equation from Eqs. (3) and (4). Fig. 1 shows the osmotic pressure (π) as a function of feed concentration (C_f) calculated from Eqs. (5)–(7) at 25°C. The differences among the calculated osmotic pressures are several bars, which is not negligible. In general, the osmotic pressure is affected by the ions composition and concentrations, which are quite site-specific. This is the reason why different osmotic pressure equations show the different calculation results as shown in Fig. 1.

As the osmotic pressure and TCF are quite site-specific, it is important to select proper equations reflecting the characteristics of feed water and RO membrane used in the field for the better normalization performance. The better normalized

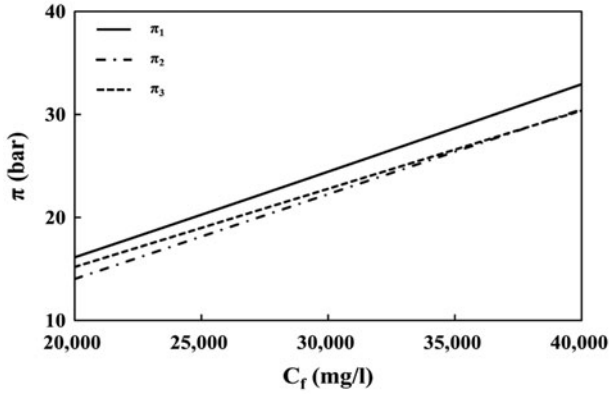

Fig. 1. The calculated osmotic pressure from various empirical equations.

performance means that the NPF data group has a lower variance (or standard deviation) during an operation period without fouling. Although the candidates for the empirical osmotic pressure equation and the temperature coefficient for water transport of the RO membrane (a in Eq. (4)) are provided, it could be better to introduce fitting equations for the feed osmotic pressure and TCF reflecting the feed water and membrane characteristics in the field. Thus, a simple formula for osmotic pressure with four unknown parameters (α, β, γ, and δ) is introduced:

$$\pi_4 = (\alpha C_f + \beta)(\gamma T + \delta) \tag{8}$$

The fitting procedure to find the unknown parameters (e.g. α, β, γ, and δ in Eq. (8); and a in Eq. (4)) of the osmotic pressure and TCF formula is a simple optimization approach by minimizing the variance (or standard deviation) of the NPF data group during the non-fouling period. The optimization approach is carried out with Microsoft excel solver. The calculated NPF with the fitted osmotic pressure and TCF equation is called corrected NPF in this work.

2.2. Statistics-based fouling detection method

The objective of the RO data normalization is literally to normalize the fouling parameter such as NPF. An ideal case of the normalization results in a constant value during a non-fouling period. Unfortunately, as discussed earlier, a normalized parameter fluctuates with a variance even in the non-fouling period. Fig. 2 shows an example of a fluctuated normalized parameter, NPF. Due to the fluctuation, it is impossible to figure out the time when fouling starts by monitoring separate NPF values. Instead, a group monitoring may make it possible to find the early state of fouling. Our hypothesis here is that a group of consecutive NPF data in a fouling-occurred period should have a statistically different mean value from a group in a non-fouling period. Thus, the two groups are defined to perform the fouling detection (Fig. 2): (1) Group A which contains the consecutive NPF data from the start of operation to the present time and (2) Group B with the recent NPF data including the present datum. Group A and Group B represent a non-fouling period and an unknown period (to be checked if fouling occurs or not), respectively. If the mean of Group B is statistically smaller than that of Group A, Group B falls in a fouling-occurred period because NPF declines.

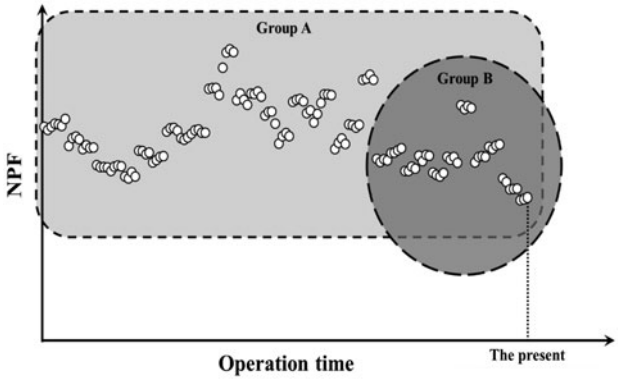

Fig. 2. The concept of the statistic-based fouling detection method.

The mean values of the two groups with different population sizes and variances are then compared using the one tailed t-test [20,23]. Fouling detection index (FDI) is defined from the result of the t-test as shown in Eq. (9) to check whether fouling starts or not.

$$\mathrm{FDI} = \frac{\mu_B - \mu_A}{\sqrt{\frac{\sigma_A^2}{n_A} + \frac{\sigma_B^2}{n_B}}} + t_{df,p} \tag{9}$$

where μ, σ, n, and t are mean, standard deviation, population size, and t statistic, respectively; and A, B, df, and p represent Group A, Group B, degree of freedom, and significance level of the t-test, respectively. The degree of freedom (df) for this t-test can be calculated by:

$$\mathrm{df} = \frac{\left(\frac{\sigma_A^2}{n_A} + \frac{\sigma_B^2}{n_B}\right)^2}{\frac{(\sigma_A^2/n_A)^2}{n_A - 1} + \frac{(\sigma_B^2/n_B)^2}{n_B - 1}} \tag{10}$$

The fouling detection time is defined as the time when FDI becomes negative for the first time. In order to avoid the false detection of fouling, the appropriate significance level (p) should be determined first. It is defined as the maximum value while FDI remains positive during a non-fouling period.

2.3. Laboratory-scale RO fouling test

In order to verify the early fouling detection method using the corrected NRF discussed in Sections 2.1 and 2.2, laboratory-scale RO fouling tests were carried out by the laboratory-scale RO experimental procedure described elsewhere [24,25]. SWRO membrane was provided by Toray Chemical, Korea,

Inc. A scientific grade marine salt mix (Coralife, Franklin, Wisconsin, USA) was used to simulate seawater. The humic acid (Waco Pure Chemical Industries, Japan) was used as a foulant.

The two types of fouling tests were carried out: (1) the constant-control test and (2) the random-control test. In the constant-control test, the operation conditions such as salt concentration, temperature, and pressure are controlled at constant values (32,000 mg/l, 24˚C, and 50 bars) from the start of the test while the random-control test is performed with randomly varied operation conditions (29,000–33,000 mg/l, 14–30˚C, and 45–50 bars). The feed salt concentration was controlled by adding the salt mix or the pure water, and the feed water temperature was controlled by a recirculating chiller. During the fouling tests, water flux was measured by weighing the permeate using a balance. Feed water conductivity and temperatures were measured by MI-180 (Martini Instrument, USA).

3. Results and discussion

3.1. Effect of fouling on flux decline

Fig. 3 shows the fouling test results from the constant-control test and the random-control test. For both fouling tests, 10 mg/l of humic acid (HA) was spiked to see the effect of fouling on flux decline. In the constant-control test where the operation conditions maintain constant values, the flux also shows very little fluctuation (21.8–22.0 LMH) until HA is spiked (Fig. 3(a)). As soon as HA is added into the feed tank, the flux suddenly drops by 7% and the fouling starting time can be easily identified.

In the random-control test where temperature, pressure, and feed total dissolved solids (TDS) concentration vary randomly as shown in Fig. 3(c), it is almost impossible to figure out the fouling starting time due to the flux fluctuation. The flux varies from 15.2 to 41.0 LMH with standard deviation of 5.8 LMH before adding HA of 10 mg/l at the operation time of 495 min, and there is no evident change in flux after HA is added. Generally, RO membrane flux increases at higher pressures, lower feed TDS concentrations, and higher temperatures when there is no fouling. As the changes in pressure and TDS are not quite large compared to temperature (Fig. 3(c)), the flux fluctuation patterns are similar to the temperature fluctuation pattern when Fig. 3(b) and (c) are compared. In order to detect fouling in the random-control test with varied operation conditions, the normalization should be carried out to distinguish the fouling situation from the normal state.

3.2. NPF and FDI

Fig. 4 presents NPF and FDI calculated from raw flux data in the random-control fouling test discussed in Section 3.1. The NPF data are produced as a result of normalization using ASTM D4516 method (Eq. (2)) with the osmotic pressure equation, π_1 (Eq. (5)), and the TCF equation, TCF_1 (Eq. (3)). Compared to the raw flux data, NPF data are clearly less fluctuated thanks to the normalization (NPF varies from 18.1 to 27.7 LMH with standard deviation of 2.3 LMH). However, it is still difficult to identify the fouling starting time (495 min) using NPF data tracking from Fig. 4(a).

In order to distinguish the fouling state from a normal state, FDI values are calculated using Eq. (9). The FDI data with various significance level of the t-test (p value) are shown in Fig. 4(b). FDI increases as p value decreases because the t statistic ($t_{df,p}$) increases at lower p values. As discussed in Section 2.2, the appropriate p value is determined to be the maximum while FDI remains positive during a non-fouling period (i.e. $p = 1.0 \times 10^{-14}$ in Fig. 4(b)). With the appropriate p value, there are no FDI values smaller than zero over entire operation times in Fig. 4(b). Since the negative FDI value means the fouling detection, the NPF using π_1 and TCF_1 fails to detect fouling. The main reason to fail is the fluctuation of NPF. Because of the fluctuation in NPF, the effect of the HA injection is covered and thus fouling cannot be discovered. Thus, better selections of the osmotic pressure and TCF equations to make less fluctuated NPF should be necessary to detect fouling with the normalized parameter, NPF, which is called the corrected NPF.

3.3. Corrected NPF for fouling detection

In order to distinguish a fouling state from a normal state, the variance in NPF in a normal state (a non-fouling period) should be minimized. It is possible to minimize the fluctuation of NPF by selecting proper osmotic pressure and TCF equations. Fig. 5 shows the effect of the osmotic pressure equations, π_1 (Eq. (5)), π_2 (Eq. (6)), π_3 (Eq. (7)), and π_4, on the calculated NPF and FDI in the random-control fouling test discussed in Section 3.1. π_4 is a fitted osmotic pressure equation with basic form in Eq. (8) such as:

$$\pi_4 = 0.000737\, C_f \tag{11}$$

where parameters in Eq. (8) (e.g. $\alpha = 7.19$, $\beta = 0$, $\gamma = 0$, and $\delta = 0.000103$) are obtained from the fitting approach to minimize the variance in NPF during a non-fouling period. As shown in Fig. 5(b), the selection of different osmotic pressure equations does not

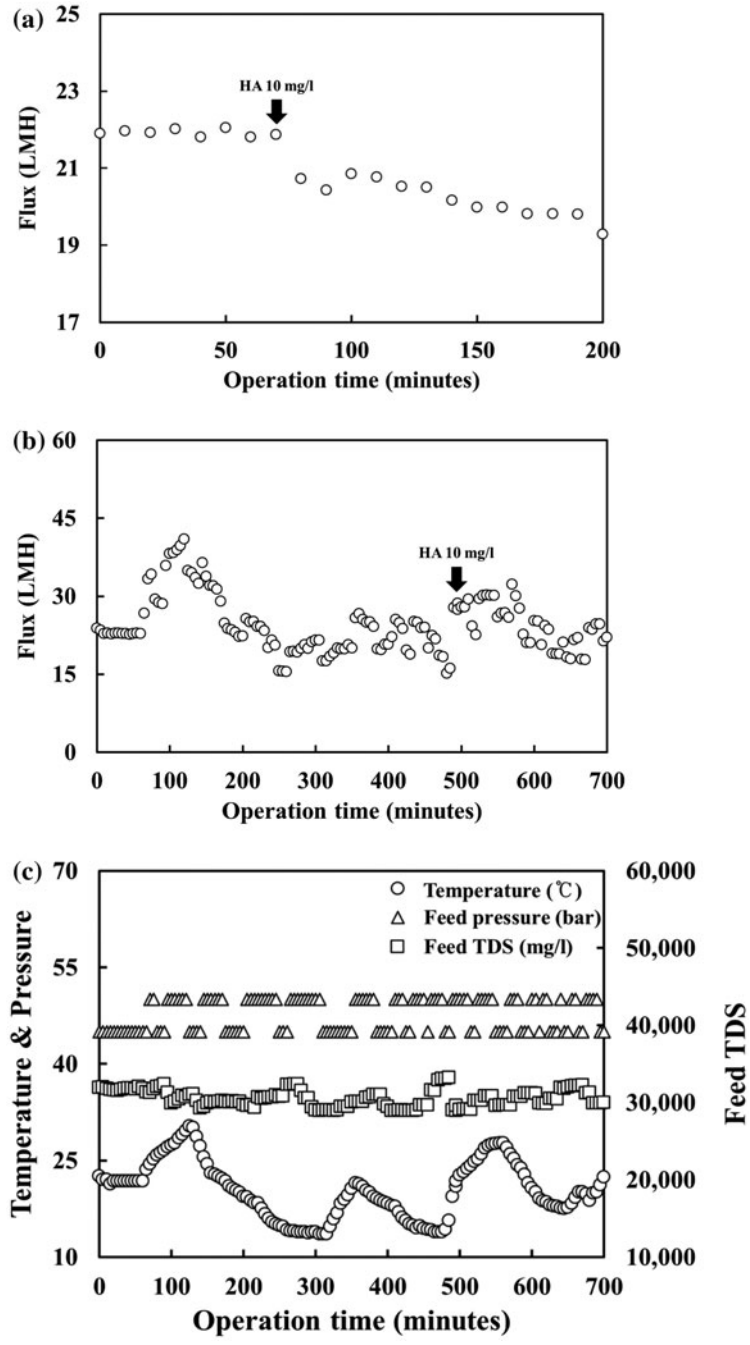

Fig. 3. Effect of fouling on flux decline in (a) constant-control test and (b) random-control test with (c) varying operation conditions such as temperature, pressure, and feed TDS concentration.

change the NPF data dramatically, and Fig. 5(c) shows that the FDI values are larger than zero over entire operation periods, which means the fouling detection method using NPF data with various osmotic pressure equations fails to detect fouling in the random-control test. As a result, it is found that the selection of osmotic pressure equation does not enhance the fouling detection performance.

Although it is hard to find out which osmotic pressure equations is the best to minimize the variance in NPF during a non-fouling period from Fig. 5(b), the variances (or standard deviations) can be compared to

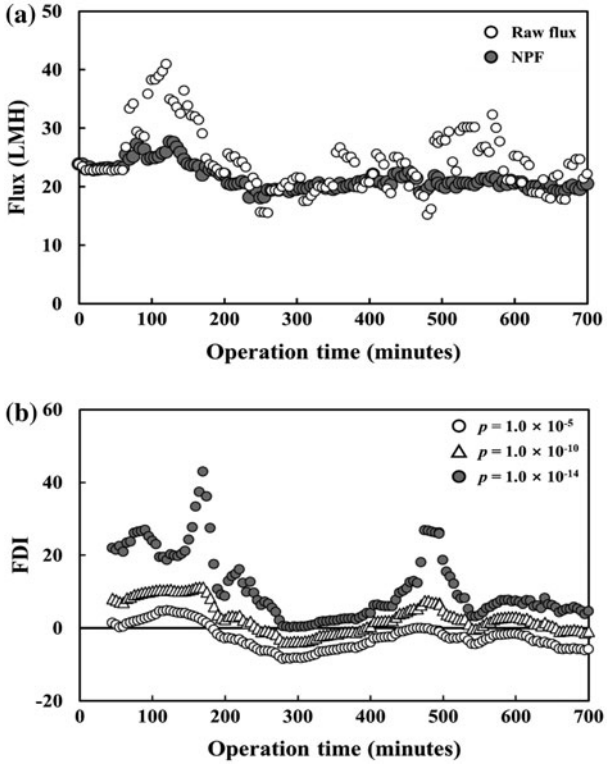

Fig. 4. (a) NPF with π_1 and TCF_1 and (b) FDI in the random-control fouling test.

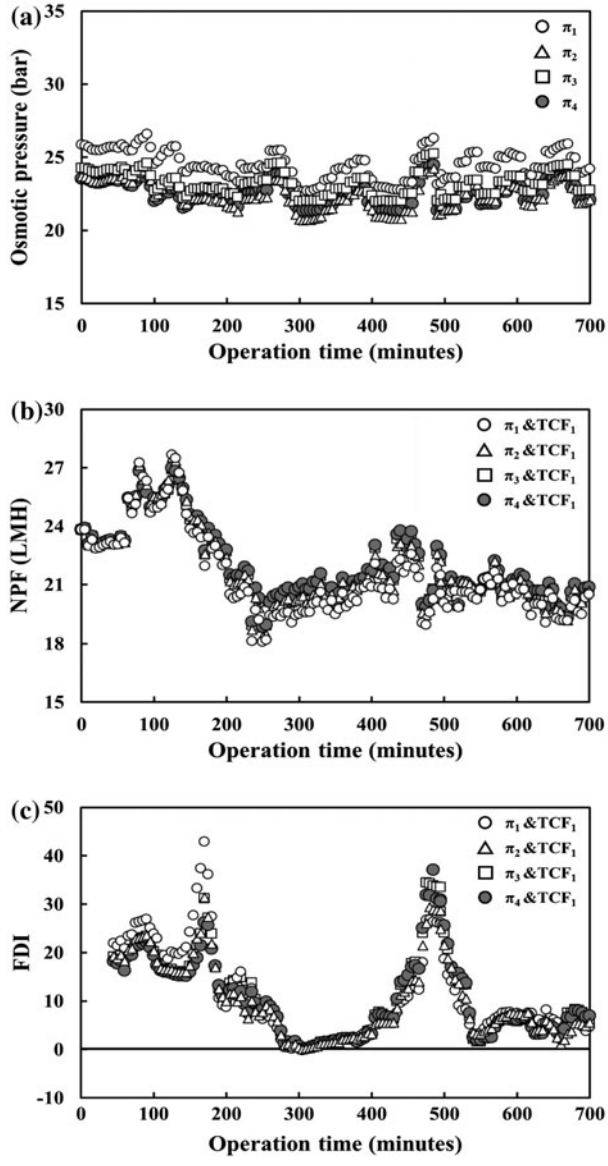

Fig. 5. Effect of (a) various osmotic pressure equations on (b) NPF and (c) FDI.

select the best osmotic pressure equation. The standard deviations of NPF data with π_1, π_2, π_3, and π_4 are 2.32, 2.21, 1.98, and 1.97 LMH, respectively. Considering π_1, π_2, and π_3 are existing equations, we found that the fitted osmotic pressure equation, π_4, is not very useful because the standard deviation of NPF with π_4 is very similar to that with π_3, one of the existing equations. Thus, π_3 can be the best osmotic pressure equation among the tested ones, and it is selected as the fixed osmotic pressure equation for the further analysis discussed below.

Fig. 6 shows the effect of various TCF equations, TCF_1 (Eq. (3)), TCF_2, and TCF_3, on the calculated NPF and FDI in the random-control fouling test. The basic form for both TCF_2 and TCF_3 is Eq. (4). The temperature coefficients for water transport for RO membrane (a) for TCF_2 and TCF_3 are 2,124 (provided by the membrane supplier), and 4,165 (the fitted parameter to minimize the variance in NPF during a non-fouling period), respectively.

The patterns of NPF with TCF_1 and TCF_2 are similar while the trend of NPF with TCF_3 is distinguished (Fig. 6(a) and (b)). The standard deviations of NPF with TCF_1, TCF_2, and TCF_3 during the non-fouling period are 1.98, 2.42, and 1.29 LMH, respectively, which means that the fitted TCF equation, TCF_3, shows the best performance in normalization. In Fig. 6(c), FDI data calculated from TCF_3 show the first negative value at the operation time of 540 min, which means that the fouling is detected at the time, 45 min after the injection of humic acid (495 min). This result indicates that the correction of TCF equation fitted for the better normalization makes it possible to succeed to detect fouling early with the statistics-based fouling detection method.

Fig. 7 shows the effect of the simultaneously fitted osmotic pressure and TCF equations (π_5 and TCF_4) on NPF and FDI compared to that of the fitted TCF

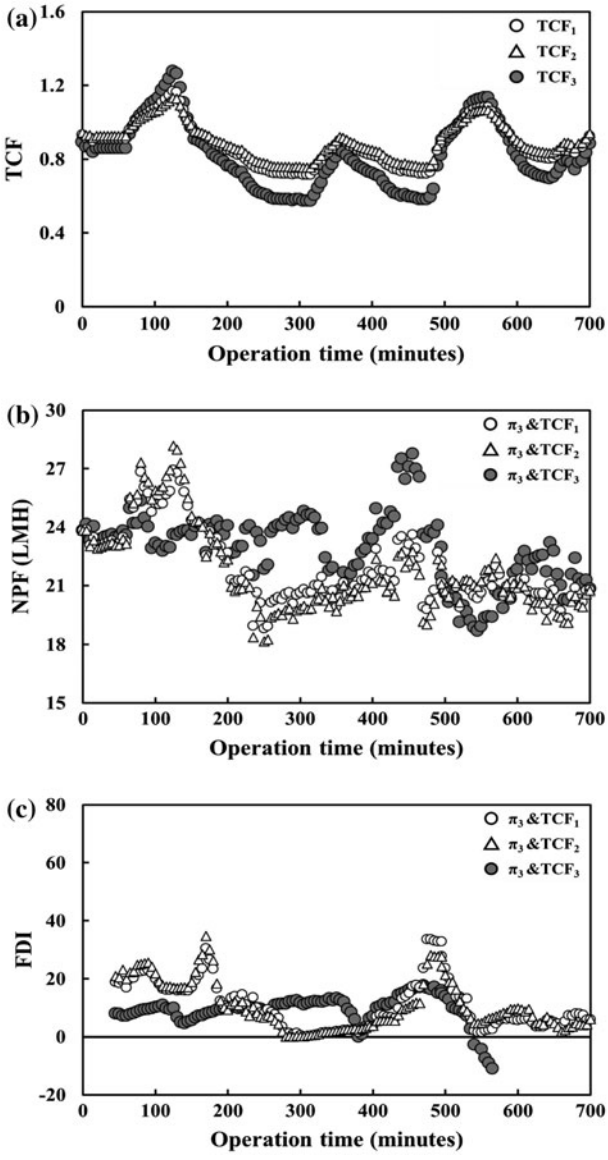

Fig. 6. Effect of (a) various TCF equations on (b) NPF and (c) FDI.

equation only (π_3 and TCF_3). Both π_5 and TCF_4 are obtained by the fitting approach to minimize the variance in NPF during the non-fouling period such as:

$$\pi_5 = 0.000782\, C_f \tag{12a}$$

$$TCF_4 = \exp\left[3830 \times \left(\frac{1}{298} - \frac{1}{T+273}\right)\right] \tag{12b}$$

As shown in Fig. 7, the simultaneous fitting procedure does not affect the performance of normalization and fouling detection at all. This result concludes that the

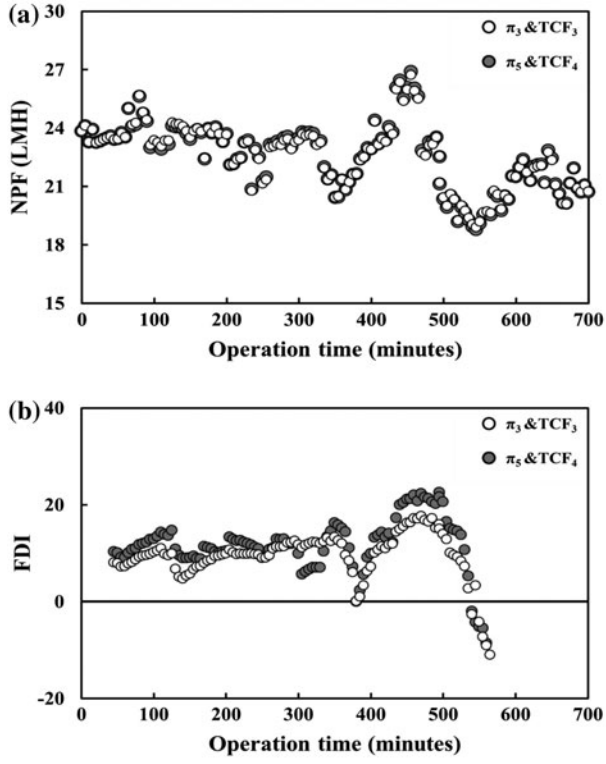

Fig. 7. (a) Corrected NPF and (b) FDI with the fitted osmotic pressure and TCF equations.

fitted TCF equation affects the performance of the normalization and the fouling detection method more than the fitted osmotic pressure equation.

4. Conclusions

Normalization is an important technique to properly operate SWRO processes because it can distinguish a fouling state from a normal state. However, the poor selection of the osmotic pressure and TCF equations which do not reflect the characteristics of feed water and RO membrane makes it difficult to detect fouling in the real-field application. Thus, this work introduced the corrected NPF and developed the statistics-based fouling detection method using it. The corrected NPF was calculated using the osmotic pressure and/or TCF equations fitted to minimize the variance in NPF during a non-fouling period (a normal state). The NPF data without using the fitted TCF equations failed to detect fouling in the laboratory-scale fouling test with randomly changing operation conditions. Thus, the fitted TCF equation affects the performance of the fouling detection method more than the fitted osmotic pressure equation. In the random-control fouling test, the corrected NPF with the

fitted TCF equation succeeded to detect fouling in 45 min after the addition of humic acid, which leads a conclusion that the statistics-based fouling detection method using the site-specific NPF will be useful to operate the SWRO processes with varied operation conditions.

Acknowledgment

This research was supported by a grant (code 15IFIP-B088091-02) from Industrial Facilities & Infrastructure Research Program funded by Ministry of Land, Infrastructure and Transport of Korean government.

References

[1] L.D. Tijing, Y.C. Woo, J.S. Choi, S. Lee, S.H. Kim, H.K. Shon, Fouling and its control in membrane distillation —A review, J. Membr. Sci. 475 (2015) 215–244.
[2] A. Jiang, L.T. Biegler, J. Wang, W. Cheng, Q. Ding, S. Jiangzhou, Optimal operations for large-scale seawater reverse osmosis networks, J. Membr. Sci. 476 (2015) 508–524.
[3] E.M.V. Hoek, J. Allred, T. Knoell, B.H. Jeong, Modeling the effects of fouling on full-scale reverse osmosis processes, J. Membr. Sci. 314 (2008) 33–49.
[4] E. Alhseinat, R. Sheikholeslami, A completely theoretical approach for assessing fouling propensity along a full-scale reverse osmosis process, Desalination 301 (2012) 1–9.
[5] S. Kim, D. Cho, M.S. Lee, B.S. Oh, J.H. Kim, I.S. Kim, SEAHERO R&D program and key strategies for the scale-up of a seawater reverse osmosis (SWRO) system, Desalination 238 (2009) 1–9.
[6] S. Kim, B.S. Oh, M.H. Hwang, S. Hong, J.H. Kim, S. Lee, I.S. Kim, An ambitious step to the future desalination technology: SEAHERO R&D program (2007–2012), Appl. Water Sci. 1 (2011) 11–17.
[7] D.V. Gauwbergen, J. Baeyens, Modelling reverse osmosis by irreversible thermodynamics, Sep. Purif. Technol. 13 (1998) 117–128.
[8] N. Melián-Martel, J.J. Sadhwani, S. Malamis, M. Ochsenkühn-Petropoulou, Structural and chemical characterization of long-term reverse osmosis membrane fouling in a full scale desalination plant, Desalination 305 (2012) 44–53.
[9] J.S. Choi, J.T. Kim, Modeling of full-scale reverse osmosis desalination system: Influence of operational parameters, J. Ind. Eng. Chem. 21 (2015) 261–268.
[10] A.H. Taheri, L.N. Sim, T.H. Chong, W.B. Krantz, A.G. Fane, Prediction of reverse osmosis fouling using the feed fouling monitor and salt tracer response technique, J. Membr. Sci. 475 (2015) 433–444.
[11] S. Kim, E.M.V. Hoek, Interactions controlling biopolymer fouling of reverse osmosis membranes, Desalination 202 (2007) 333–342.
[12] S. Lee, S. Kim, J. Cho, E.M.V. Hoek, Natural organic matter fouling due to foulant-membrane physicochemical interactions, Desalination 202 (2007) 377–384.
[13] X. Jin, A. Jawor, S. Kim, E.M.V. Hoek, Effects of feed water temperature on separation performance and organic fouling of brackish water RO membranes, Desalination 239 (2009) 346–359.
[14] S. Kim, S. Lee, E. Lee, S. Sarper, C.H. Kim, J. Cho, Enhanced or reduced concentration polarization by membrane fouling in seawater reverse osmosis (SWRO) processes, Desalination 247 (2009) 162–168.
[15] S. Kim, S. Lee, C.H. Kim, J. Cho, A new membrane performance index using flow-field flow fractionation (fl-FFF), Desalination 247 (2009) 169–179.
[16] S. Kim, Osmotic pressure-driven backwash in a pilot-scale reverse osmosis plant, Desalin. Water Treat. 52 (2014) 580–588.
[17] Dow liquid separations, Filmtec reverse osmosis membranes technical manual, The Dow Chemical Company Form No. 609-00071-0705, 2005.
[18] M.A. Amin Saad, Early discovery of RO membrane fouling and real-time monitoring of plant performance for optimizing cost of water, Desalination 165 (2004) 183–191.
[19] M. Safar, M. Jafar, M. Abdel-Jawad, S. Bou-Hamad, Standardization of RO membrane performance, Desalination 118 (1998) 13–21.
[20] S. Kim, Realtime sensing method for membrane abnormal state, Korea Patent No. 1020150061630, 2015 (pending).
[21] ASTM, Standard Practice for Standardizing Reverse Osmosis Performance Data, D 4516-00 American Society for Testing and Materials, West Conshohocken, 2010.
[22] A.M. Hoffman, Design Guidelines for a Reverse Osmosis Desalination Plant, Doctoral dissertation. North-West University, Potchefstroom, 2008.
[23] P. Berthouex, L. Brown, Statistics for Environmental Engineers, Lewis Publishers, Florida, 2002.
[24] M. Kim, M. Kim, B. Park, S. Kim, Changes in characteristics of polyamide reverse osmosis membrane due to chlorine attack, Desalin. Water Treat. 54 (2015) 923–928.
[25] B. Park, J. Lee, M. Kim, Y.S. Won, J.H. Lim, S. Kim, Enhanced boron removal using polyol compounds in seawater reverse osmosis processes, Desalin. Water Treat. 57 (2016) 7910–7917.